Condition assessment of two prestressed concrete slabs after 60 years in service

Dana Tawil[1,*], *Leah* Kristufek[1], *Beatriz* Martin-Perez[1] , *Leandro* F.M Sanchez[1], and *Martin* Noël[1]

[1]Department of Civil Engineering, University of Ottawa, Ottawa, ON K1N 6N5, Canada

Abstract. Two concrete deck slabs extracted from a Canadian bridge have been evaluated using non-destructive testing (NDT), followed by destructive testing. Throughout its service life, the bridge experienced harsh environmental conditions with frequent freeze-thaw cycles, hot and humid summers, and the use of de-icing salts during winters. This study presents the preliminary results of an exhaustive condition assessment of two prestressed concrete slab panels, where NDT techniques (visual assessments, electrochemical and concrete soundness tests) have been conducted prior to destructive testing. Although visual inspection did not indicate poor concrete quality, the results of the ultrasonic pulse velocity testing showed that both concrete slabs are of poor quality and may be suffering from internal defects. Chlorides may have also been introduced through the strand conduit anchor points. These findings raise concerns regarding the structural integrity of corrosion-affected members.

1 Introduction

Bridges in Canada are subjected to harsh climates, winter de-icing salts, increasing traffic demand, as well freeze-thaw cycles. After several decades, elements of these concrete bridges show significant signs of deterioration. This paper presents the results of visual inspection and non-destructive testing of two elements obtained from one of these bridges.

The superstructure's deck design (Fig. 1), which included transversely prestressed concrete infill slabs, introduced problems when replacing deteriorated members or monitoring their structural health.

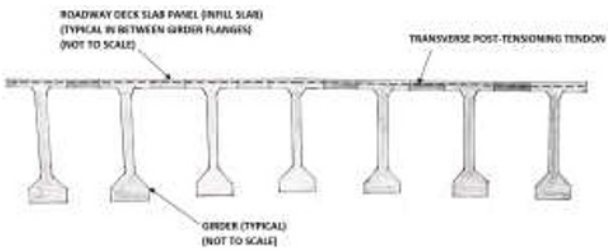

Fig. 1. Typical cross-section of concrete deck span.

This bridge was built during a crucial time in the evolution of bridge construction techniques and winter road maintenance practices. Winter runoff, which contains chlorides from de-icing salts, was not considered in the design of the bridge components. Moreover, the use of air entrainers to prevent freezing and thawing cycles was still being developed at the time the bridge was constructed. This made concrete utilized during this time more susceptible to freeze-thaw cycles. As a result, many concrete structures built between the 1960's and 1980's, similar to this bridge, are showing major signs of distress at a quicker rate than expected [1, 2].

As part of the highly integrated superstructure, the infill slabs (Fig. 2) play a major role in the bridge's load-transfer system. The continuous use of de-icing salts over the lifespan of the bridge, combined with the failure to incorporate appropriate mitigation measures, such as proper drainage systems, contributed to the corrosion of the slabs' post-tensioned prestressing tendons. The close proximity of the infill slabs to traffic may have increased their exposure to carbon monoxide, leading to concrete carbonation and the gradual decrease of the pH level in the concrete cover. The combined effects of their exposure to carbonation and chloride ions may have accelerated the rate of corrosion.

Although extensive progress in this field has been achieved throughout the years, available research has mainly focused on determining the material deterioration and structural implications of concrete elements suffering from reinforcement corrosion by conducting laboratory experimental testing [3-5]. However, laboratory test samples typically experience free-expansion conditions, while field members undergo a variety of stress-state and confinement conditions. As a result, it is of great importance to fully understand how distress mechanisms, such as corrosion, influence the mechanical, durability

* Corresponding author: dalta085@uottawa.ca

and functional properties of affected ageing concrete field members over time.

A) S1 soffit.

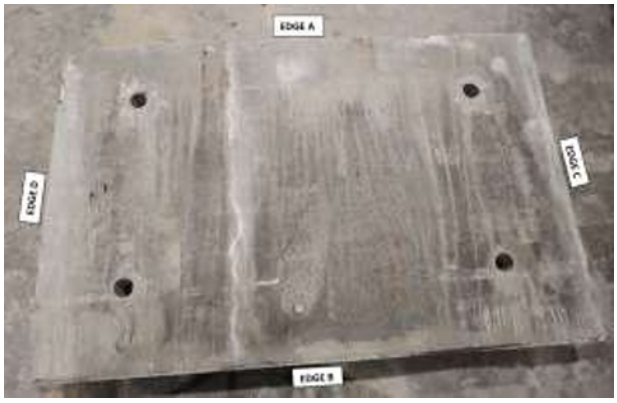

B) S7 soffit.

Fig. 2. Infill slabs extracted from the bridge: A) S1 and; B) S7.

2 Scope of work

This work is part of a broader evaluation of the bridge, which includes the diagnosis and prognosis of various extracted structural elements, and the establishment of management protocols for bridges in similar climates. This paper focuses on the condition assessment of two prestressed concrete infill slabs, S1 and S7 (Fig. 2), which have been exposed to aggressive environmental conditions for several years. The objective of the work is to correlate the material deterioration and structural implications of corrosion by evaluating field members extracted from an actual structure. A detailed multi-scale study, which includes a wide range of in-situ and laboratory techniques, were conducted to evaluate the infill slabs. The intent is to establish a link between corrosion-induced damage with the micro-environment and field loading conditions.

3 Methodology

The 2 m x 3 m concrete infill slabs described in this study were received by the authors in late 2021 and stored in an indoor laboratory since February 2022. Non-destructive tests listed in Section 4 have been completed at the indoor storage location. Visual inspection aided in qualitatively identifying areas of concrete spalling, delamination, and cracking. The remaining tests listed in Section 4 identified any sub-surface defects, as well as the possibility of corrosion within the embedded prestressing and regular reinforcing steel. Further tests, including the stiffness damage test (SDT), damage rating index (DRI), compressive strength test, titration testing for chloride concentrations, testing for carbonation, four-point bending test, and tensile and gravimetric tests of the extracted tendons will be performed in the near future. The results of these tests will aid in evaluating the extent of corrosion, as well as its structural implications. Numerical modelling will also be conducted to assess the slab structural integrities by investigating the effects of damage localization, load-sharing, and the reduction in the transverse prestressing level.

4 Results and discussion

4.1. Visual assessment

The slabs were cut from the driving surface of the bridge without removing the asphalt pavement (Fig. 3). All grouted post-tensioning tendons are composed of 12-7 mm diameter strands tightly grouped within a metal duct. The application of grout for all tendons appears successful, with limited visible empty space between the individual strands and between the tendon and duct (Fig. 4). Few strands appear to be centred within the duct, while the remaining strands have shifted to the sides. Tendon labelling refers to the slab the tendon is embedded in, the slab edge from which it is visible, and the tendon number. For example, S1A1 and S1B1 refer to tendon 1 observed from edges A and B of slab S1, respectively. Temperature reinforcement (15-mm diameter bars) is located along the longitudinal slab directions. Concrete damage along the slab edges occurred when relocating the specimens. Table 1 summarizes the main results of the visual inspection.

A) S1 elevation.

B) S7 elevation.

Fig. 3. Elevation view of infill slabs: A) S1 and; B) S7 with exposed soffit.

A) S1 tendons B) S7 tendons

Fig. 4. Cross-sectional view of tendons along edges A and B of: A) S1 and; B) S7.

4.2. Non-destructive tests

4.2.1 Schmidt rebound hammer and ultrasonic pulse velocity

The rebound hammer is a testing apparatus used to evaluate the hardness of concrete. The rebound number was determined along three transverse strips located at 500 mm, 1,500 mm, and 2,500 mm intervals from the edge of the soffits. Four areas were tested as per ASTM C805 along each strip using the original Proceq Schmidt rebound hammer device [6] (Fig. 5). The instrument was held in a vertical – downward position, forming a 90º angle with the horizontal. The average rebound numbers for S1 and S7 were 54.84 and 55.39, respectively, with coefficients of variation ranging between 1.1% and 4.8%. These results indicate that both slabs have similar concrete hardness.

The ultrasonic pulse velocity (UPV) method was also utilized to measure the propagation velocity of longitudinal stress-wave pulses over a known path length [7]. This technique determines the uniformity and quality of concrete. The UPV method was performed along 15-800 mm longitudinal strips that are bounded by the steel reinforcement and the transverse prestressing tendons (Fig. 6). The Screening Eagle Pundit UPV device was utilized for this test. UPV values for both slabs ranged between 2.0 km/s and 2.8 km/s, with coefficients of variation ranging between 2.6% and 19.4%. The results indicate that both slabs have poor concrete quality [8]. This could likely be due to internal defects.

The combined Sonic Rebound (SonReb) method was then utilized to determine the concrete compressive strength. This method combines the results obtained from both the Schmidt rebound hammer and the UPV values and is the most common non-destructive approach for concrete strength assessment. Many empirical formulations have been established throughout the years to determine the concrete compressive strength with the SonReb method. Seventeen formulations, discussed by Cristofaro et al. (2020) [9], representing an important sample of the predictive models proposed so far have been evaluated.

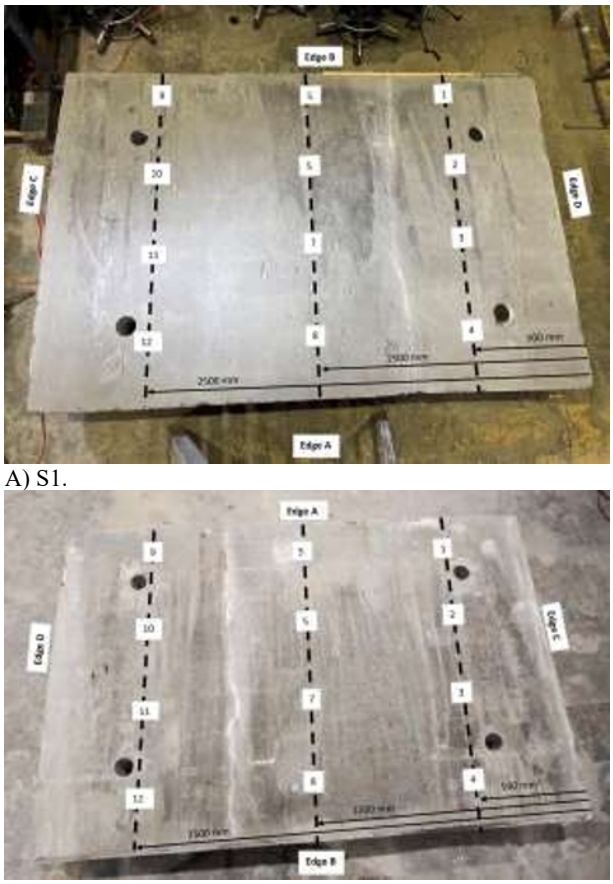

A) S1.

B) S7.

Fig. 5. Rebound hammer test areas on A) S1 and; B) S7.

Table 1. Visual inspection results from infill slabs S1 and S7.

Infill slab	Number of transverse tendons	Average spacing of tendons (cm)	Average spacing of longitudinal reinforcement (cm)	Surface cracks	Direction of cracks	Maximum crack opening (mm)	Signs of efflorescence
S1	2	103.7	20.3	At tendon locations	Transversally along direction of tendons	0.1	Along one crack (above S1A1- S1B1)
S7	4	99.7	20.4	At tendon locations	Transversally along direction of tendons	0.1	Along one crack (above S7A2-S7B2)

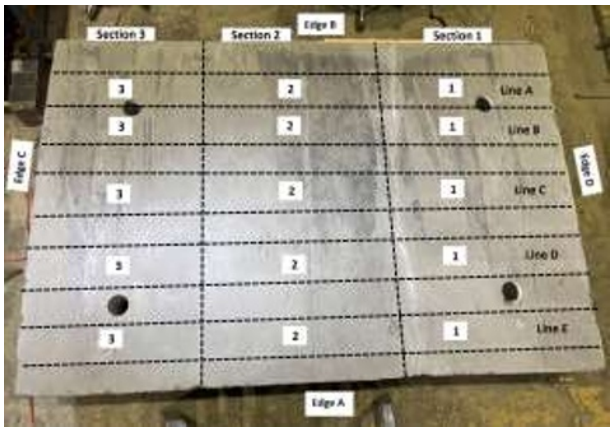

A) S1

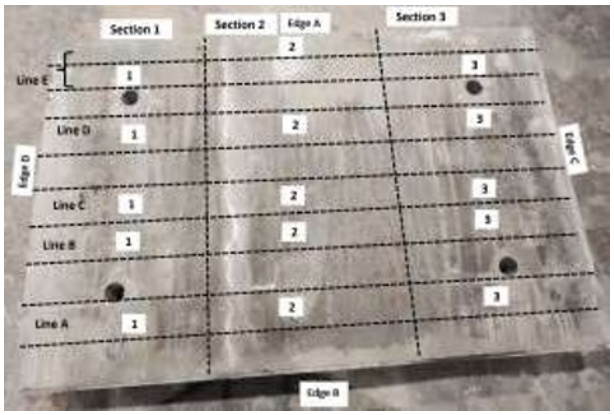

B) S7

Fig. 6. UPV test areas on A) S1 and; B) S7.

The formulations were developed by utilizing different concrete cubes and cylinders prepared in the laboratory. The majority of the proposed equations underestimated the concrete compressive strengths of the slabs. The following empirical formulation developed by Meynink and Samarin (1979) [10] was found to provide concrete compressive strengths that fall within an acceptable range of the reported concrete design strengths:

$$f_{cyl} = -24.1 + 1.24(I_r) + 0.058(V_{us})^4 \quad (1)$$

where f_{cyl} is the cylindrical concrete strength (MPa), I_r is the average rebound number, and V_{us} is the average pulse velocity (km/s).

The calculated compressive strengths for S1 and S7, 44.23 MPa and 45.0 MPa, respectively, are in accordance with the reported concrete design strength of 40 MPa.

4.2.2 Testing for corrosion

Interior prestressing tendons and steel reinforcement were evaluated using half-cell potential measurements. This method determines the voltage between the prestressing tendons or reinforcement within the concrete and an electrode placed on the concrete's surface [11]. The Giatec iCOR device was utilized in this test to obtain an estimate of the electrical corrosion potential. Measurements were obtained at 50 cm intervals along the length of the reinforcing steel. Half-cell potential contour maps for the prestressing tendons and steel reinforcement of S1 and S7 are shown in Fig. 7 and Fig. 8.

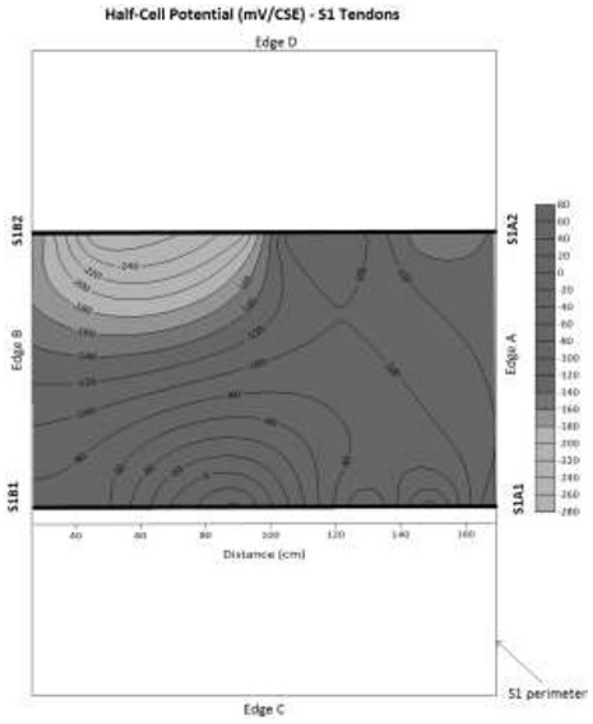

A) S1 prestressing tendons

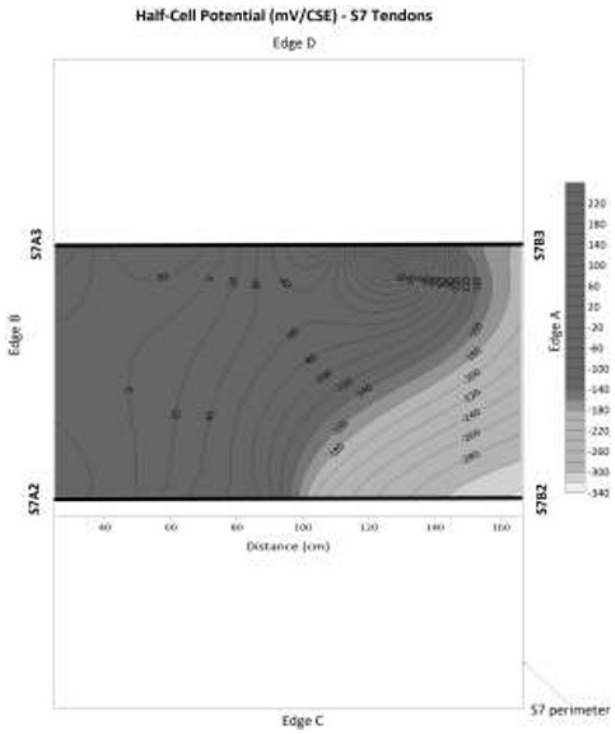

B) S7 prestressing tendons

Fig. 7. Half-cell potential mapping of prestressing tendons for A) S1 and; B) S7.

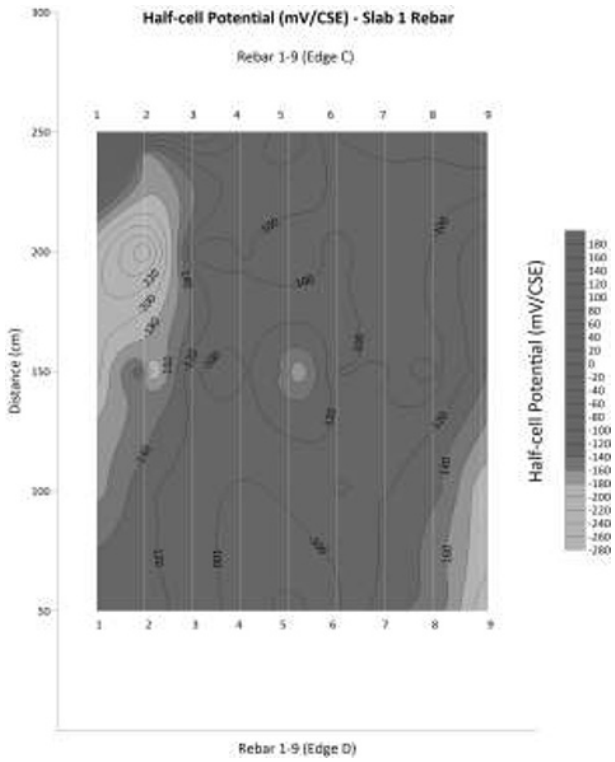

A) S1 steel reinforcement

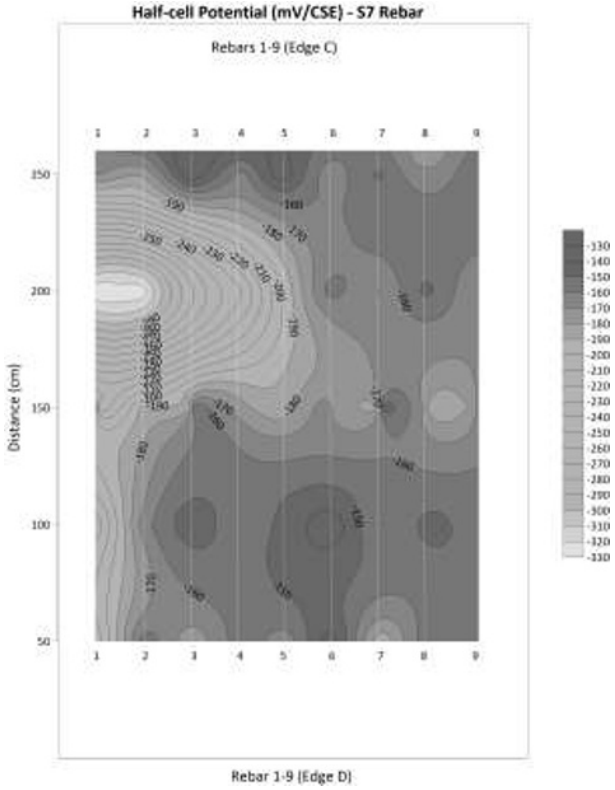

B) S7 steel reinforcement

Fig. 8. Half-cell potential mapping of reinforcing steel for A) S1 and; B) S7.

As per ASTM C876 [11], the probability of active corrosion sharply increases for S7B2 at locations near edge A. In addition, there is an uncertainty in the likelihood of corrosion for S1B2 at locations near edge B. However, the remaining prestressing tendons of S1 and S7 have a low probability of corrosion. The likelihood of corrosion for rebar 1 of S7 is high at locations near edge C, but is inconclusive at other locations along the slab. In addition, the likelihood of corrosion for rebar 2 through 5 of S7, and rebar 1 and 2 of S1 is inconclusive at locations near edge C. Rebar 9 of S1 also has an uncertain probability for corrosion near edge D. Remaining rebars from both slabs have low probabilities of corrosion. It is important to note that the metal conduit around the prestressing tendons may impact half-cell potential readings. This will be investigated at future stages of this study.

4.2.3 Testing for chlorides and carbonation

Preliminary colorimetric testing for chlorides and carbonation was performed on S1 and S7. Clear silver nitrate ($AgNO_3$) solution, at 0.1 mol/L concentration, was sprayed over the recently fractured concrete edges of both slabs. This technique allows the identification of chloride ions within the concrete. Silver ions (Ag^+) react with the free chloride ions (Cl^-) to form silver chloride (AgCl), which results in white precipitation [12]. The results of this test indicated the presence of chlorides around S1A1 and S1B2 within the metal conduit, as well as in the concrete crack located above S1A1-S1B1 (Fig.

9). Similar observations were noted for S7B1 and the concrete crack above this strand (Fig. 10). The presence of chlorides at these locations suggests that corrosion was initiated by chlorides introduced at tendon anchor points in the deck system.

A) S1A1

B) S1B2

C) Along concrete crack above S1A1-S1B1

Fig. 9. Testing for chlorides with silver nitrate solution on S1: A) S1A1, B) S1B2 and; C) concrete cracking above S1A1-S1B1.

A) S7B1

B) Along concrete crack above S7A1-S7B1

Fig. 10. Testing for chlorides with silver nitrate solution on S7: A) S7B1, and; B) concrete cracking above S7A1-S7B1.

Phenolphthalein spray solution is a method that is used to identify and measure carbonation depths in concrete. When the colourless solution comes in contact with a fresh fractured concrete surface of high pH value, the solution turns purple [12]. This technique captures the colour change between uncarbonated and carbonated concrete [13]. The test was applied on freshly cut surfaces of both slabs. No colour change was observed for both surfaces. Further testing will be performed at future stages of this study in order to determine the pH values at varying concrete depths.

5 Conclusions

Based on the above obtained results, the following conclusions can be drawn:

- The concrete compressive strengths of S1 and S7 obtained using the SonReb method are in accordance with the reported concrete design strength.

- Although visual inspection did not indicate poor concrete quality, UPV testing suggests that both concrete slabs are of poor quality, with the possibility of suffering from internal defects. As a result, it is expected that cores extracted from these elements will reveal internal defects.
- The results obtained from corrosion measurements and preliminary colorimetric testing highlight that chlorides may have been introduced through the strand conduit, specifically at anchor points that connected the infill slabs to the top flanges of the girders.

The condition assessment of the two prestressed concrete slabs is currently ongoing. Upcoming work includes cutting the slab in preparation for four-point bending tests and core extractions for destructive tests, as well as numerical modelling using finite element analysis. In addition, chloride ion concentrations will be determined by titration. The effects of the metal conduit on the half-cell potential readings of the strands will also be examined.

References

1. K. Mermigas. *2018 Conf. Transp. Assoc. Canada* (2018)
2. L. F. M. Sanchez, B. Fournier, D. Mitchell, and J. Bastien. Constr. Build. Mater., 236, 117554 (2020)
3. B. Cousin, B. Martín-Pérez. *6th Int. Conf. on Concr. under Severe Cond.: Env. and Load.,* pp. 247–256 (2010)
4. A. K. Azad, S. Ahmad, S. A. Azher. ACI Mater. J. **104**, pp. 40–47 (2007)
5. Z. Rinaldi, S. Imperatore, C. Valente. Constr. Build. Mater. **24**, pp. 2267–2278 (2010)
6. ASTM C 805-02. *Standard Test Method for Rebound Number of Hardened Concrete*. (United States Am. Soc. Test. Mater. 2002)
7. ASTM C 597-02. *Standard test Method for Pulse Velocity Through Concrete*. (United States Am. Soc. Test. Mater. 2003)
8. E. A. Whitehurst. Am. Concr Inst., pp. 94 (1996)
9. M.T Cristofaro, S. Viti, M. Tanganelli. J. Build. Eng. **27**, 100962 (2020)
10. P. Meynink, A. Samarin, *RILEM Symp. Proc. Qual. Control Concr. Struct*, pp. 127–134 (1979)
11. ASTM C876-15. *Standard Test Method for Corrosion Potentials of Uncoated Reinforcing Steel in Concrete*. (United States Am. Soc. Test. Mater. 2017)
12. C. V. Pontes, GC Réus, EC Araújo, MHF Medeiros. J. Build. Eng., pp. **34**, 101860 (2020)
13. Y. Lo, & H.M. Lee. Build. and Environ. **37**, pp. 507–514 (2002)